AD-A121 575 NANOSECOND PULSER THYRATRONS(U) EG AND G INC SALEM MA 1/1
S FRIEDMAN AUG 82 DELET-TR-80-0282-3 DAAK20-80-C-0282

UNCLASSIFIED F/G 9/1 NL

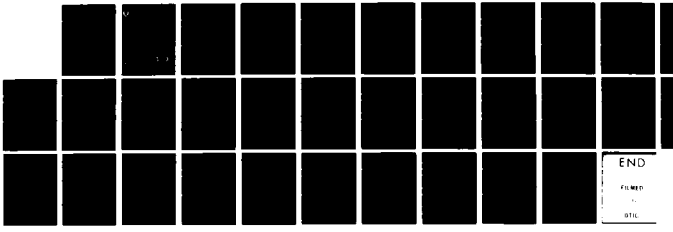

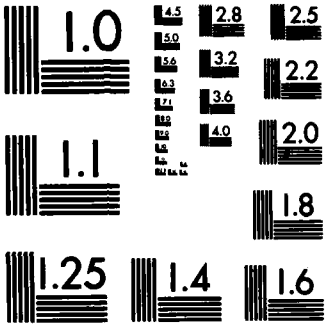

(12)

Research and Development Technical Report
DELET-TR-80-0282-3

AD A121575

NANOSECOND PULSER THYRATRONS

Steven Friedman

EG&G, INC.
35 Congress Street
Salem, MA 01970

August 1982

Third Interim Report for Period 1 August 1981 — 30 December 1981

DISTRIBUTION STATEMENT

Approved for public release;
distribution unlimited.

Prepared for:
Electronics Technology & Devices Laboratory

ERADCOM

U.S. ARMY ELECTRONICS R&D COMMAND, FORT MONMOUTH, NEW JERSEY 07703

82 11 03 021

NOTICES

Disclaimers

The citation of trade names and names of manufacturers in this report is not to be construed as official Government endorsement or approval of commercial products or services referenced herein.

Disposition

Destroy this report when it is no longer needed. Do not return it to the orginator.

UNCLASSIFIED

SECURITY CLASSIFICATION OF THIS PAGE (When Data Entered)

REPORT DOCUMENTATION PAGE		READ INSTRUCTIONS BEFORE COMPLETING FORM
1. REPORT NUMBER: DELET-TR-80-0282-3	2. GOVT ACCESSION NO.: AD-A112157	3. RECIPIENT'S CATALOG NUMBER: 5
4. TITLE (and Subtitle): Nanosecond Pulser Thyratrons		5. TYPE OF REPORT & PERIOD COVERED: Third Interim, 1 Aug 81 - 30 Dec 81
		6. PERFORMING ORG. REPORT NUMBER
7. AUTHOR(s): Steven Friedman		8. CONTRACT OR GRANT NUMBER(s): DAAK20-80-C-0282
9. PERFORMING ORGANIZATION NAME AND ADDRESS: EG&G, Inc., 35 Congress Street, Salem, MA 01970		10. PROGRAM ELEMENT, PROJECT, TASK AREA & WORK UNIT NUMBERS: 62705, 1L162705 AH94.01.03
11. CONTROLLING OFFICE NAME AND ADDRESS: Electronics Technology and Devices Lab (ERADCOM), ATTN: DELET-PL, Fort Monmouth, NJ 07703		12. REPORT DATE: August 1982
		13. NUMBER OF PAGES: 38
14. MONITORING AGENCY NAME & ADDRESS (if different from Controlling Office)		15. SECURITY CLASS. (of this report): Unclassified
		15a. DECLASSIFICATION/DOWNGRADING SCHEDULE

16. DISTRIBUTION STATEMENT (of this Report)

Approved for public release; distribution unlimited.

17. DISTRIBUTION STATEMENT (of the abstract entered in Block 20, if different from Report)

18. SUPPLEMENTARY NOTES

19. KEY WORDS (Continue on reverse side if necessary and identify by block number)

Pulser
Nanosecond
Thyratron
Pulse Sharpener
Capacitor

20. ABSTRACT (Continue on reverse side if necessary and identify by block number)

Significant progress has been made in developing the individual circuit components for the nanosecond pulser, these being the thyratron, load, PFN, and saturable reactor.

A modified version of the HY-3013L thyratron has demonstrated substantially greater voltage holdoff and reduced triggering requirements. New recovery measurements, with circuitry designed to eliminate false

DD FORM 1 JAN 73 1473 EDITION OF 1 NOV 65 IS OBSOLETE

UNCLASSIFIED

SECURITY CLASSIFICATION OF THIS PAGE (When Data Entered)

triggering of the pulsed voltage sources, have yielded de-ionization times well within the 50us required for 20kHz operation, at voltages and pressures well beyond those needed to meet the load voltage rise time and pulse width requirements. An instant-start dispenser cathode suitable for use with HY-3013L-type thyratrons has been developed and tested successfully in similar tubes.

An ultra low inductance PFN/load combination has been constructed, and has produced a smooth 3.5ns FWHM multi-kilovolt pulse across a nominal 50pf load capacitance when switched via a short air gap. The kapton capacitors and ceramic resistor load shunt are theoretically capable of operating at around 200 watts average power.

Three saturable reactor materials have been evaluated theoretically: orthonol, metglas and ferrite. Of these, only ferrite appears usable on a 10ns time scale, metglas and orthonol being unsuitable because of their low resistivity.

Finally, a 20kHz kit has been constructed for high prr testing of the assembled nanosecond pulser circuit.

TABLE OF CONTENTS

ABBREVIATIONS AND SYMBOLS

A	Amperes (DC)
A_m	Magnetic cross-sectional area of saturable reactor material
B_S	Saturation flux density
C	Load capacitance
C_O	Storage capacitor capacitance
d,l,w	Saturable reactor assembly dimensions
DBV	Dynamic breakdown voltage
EIA	Extended interaction amplifier
epy	Thyratron charging voltage
FWHM	Full width at half maximum
i	Current
ib	Peak thyratron current
ka	Kiloamperes (pulsed)
kHz	Kilohertz
kv	Kilovolts (pulsed)
KV	Kilovolts (DC)
L	Inductance
nH	Nanohenries
ns	Nanoseconds
pd	Torr-centimeters
pF	Picofarads
prr	Pulse repetition rate
t_f	Thyratron anode fall time
t_r	Thyratron recovery time
μF	Microfarads
μs	Microseconds
V	Load voltage (DC)
V_B	Bias voltage (DC)
x	Magnetic saturation front penetration depth
ρ	Resistivity

LIST OF ILLUSTRATIONS

1 FOREWORD

This is the Third Interim Technical Report for a program of research and development conducted under ERADCOM Contract DAAK20-80-C-0282 entitled "Nanosecond Pulser Thyratrons," and covers the period 1 August 1981 to 30 December 1981.

The work described herein was performed by EG&G, Inc., Electronic Components Division, 35 Congress Street, Salem, Massachusetts 01970.

2 ELECTRICAL REQUIREMENTS OF THE EIA, OVERALL PULSER CIRCUIT, AND THYRATRON

During the period covered by this Interim Report, the Type II requirements for the nanosecond pulser circuit were changed. The peak forward voltage was reduced from 6 kv to 3.5 kv, and the load capacitance was reduced from 60 pF to 30 pF.

Using these values in the lumped circuit analysis of the Appendix (reprinted from the Second Interim Report) gives 17 nH and 5 kv for the total circuit inductance and thyratron voltage required to generate a 4 ns FWHM load voltage pulse. The load resistance required across the 30 pF comes out to be 13 ohms.

An effective increase in load voltage rise rate, as well as an effective decrease in pulse width, can be obtained by biasing the EIA grid negative with respect to the EIA cathode by voltage V_B, and then applying a pulse of magnitude V_B + 3.5 kv. The EIA will not generate any power during the initial slow-rising portion of the pulse, so that for operational purposes, only the fast, narrow upper 3.5 kv constitutes the applied voltage. The sharpening effect of this is illustrated in Figure 1. Work reported in the Second Interim Report showed that this technique will probably be necessary to achieve the required load voltage rise time and pulse width. A safe maximum value for V_B is 1.5 KV, so the total pulse voltage would be 5 kv. From the Appendix, the thyratron voltage would then be 7 kv, but experiments described in Section 4 suggest that in practice 10 kv will be required.

In summary, conservative calculations give 17 nH and 10 kv as the circuit inductance and thyratron voltage, respectively, required to generate a 3.5 kv, 4 ns voltage pulse across a 30 pF load.

Thyratrons and PFN/load circuits capable of meeting these requirements have been constructed, and are described in Sections 3 and 4. Succeeding sections describe the saturable reactor, the overall circuit, and our plans for characterizing the circuit at low and high prr.

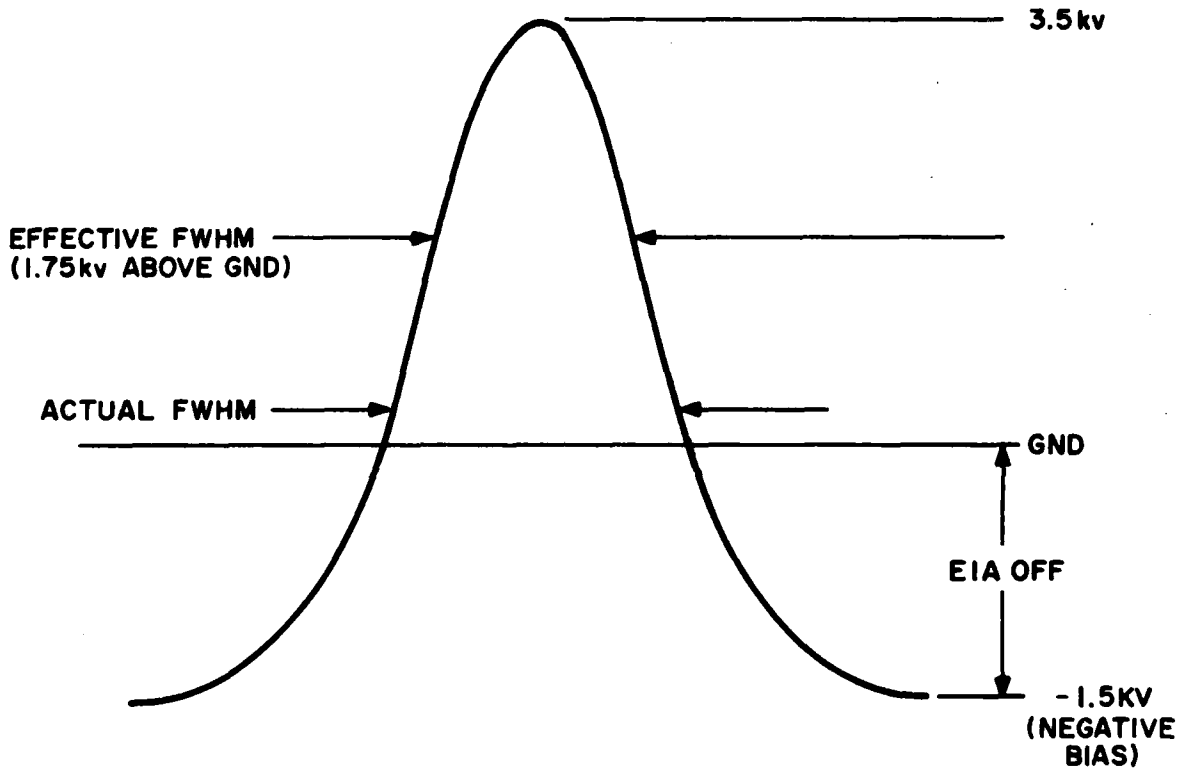

Figure 1. Reduction of effective pulse width by use of negative bias.

3 THYRATRON DEVELOPMENT

a. Voltage Holdoff

When HY-3013L (Figure 2a) was originally characterized, the load voltage specification was 6 kv. Our plan for achieving the required 1 ns voltage rise time was to operate the thyratron at high pressure, use a saturable reactor, and avoid the slow-rising early part of the pulse by using the top 6 kv of a 10 kv pulse. The resulting thyratron holdoff requirement was 15-20 kv, at 0.7 torr minimum. The DBV (dynamic breakdown voltage) vs pressure plots of Figure 3 show that HY-3013L would have satisfied this only marginally. We therefore proceeded to construct new thyratrons designed for better holdoff.

Since it was believed that the maximum holdoff of HY-3013L was limited to 20 kv by some type of field emission, we did not expect to substantially exceed this voltage. Rather, the intention was to shift the DBV curves to higher pressure, thereby decreasing the current rise time and in turn allowing operation with a pulse having a smaller total voltage.

To accomplish this, the E-E spacing was reduced to 0.050 inch (from 0.080), thus decreasing "pd." Also, the grid and grid baffle aperture widths were reduced to 0.060 inch (from 0.080). Two such thyratrons were constructed, HY-3013L2 and HY-3013L3 (Figures 2b,c).

The resulting DBV curves are plotted in Figure 3. A shift to higher pressure did in fact occur, but only by 10%. More importantly, the holdoff at pressures below 0.95 torr was dramatically higher, indicating that the DBV of HY-3013L was probably being limited by factors not related to its basic design.*

Meanwhile, progress in EIA design had also resulted in the load voltage specification being reduced to 3.5 kv across 30 pF (from 6 kv across 60 pF), thus reducing the projected thyratron holdoff requirements to 10 kv.

Thus, barring severe degradation of holdoff at high prr, all three thyratrons should easily meet the voltage and pressure requirements, with HY-3013L2 and HY-3013L3 being operable at pressures approaching 1 torr. The advantage of such high pressure operation is that the thyratron resistive fall time is reduced, thereby decreasing the anode dissipation as well as the anode current delay time which the saturable reactor must provide. (This second effect reduces the volume

---

*These factors can include small surface irregularities on the grid, anode, or ceramic insulator, evaporation of cathode coating into the high voltage region during activation, and incomplete aging. The holdoff of HY-3013L will likely improve with additional aging.

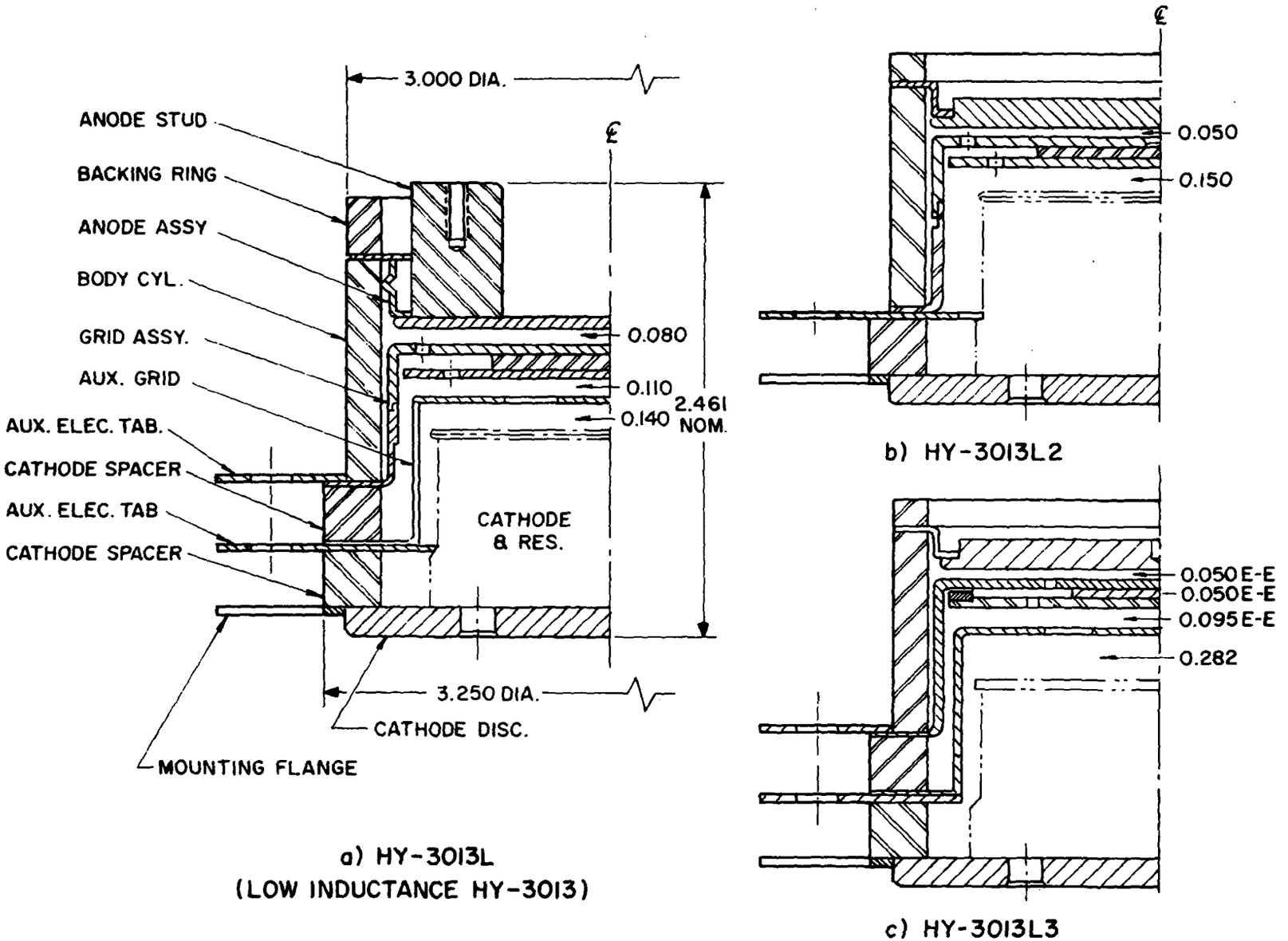

Figure 2. Low inductance tubes.

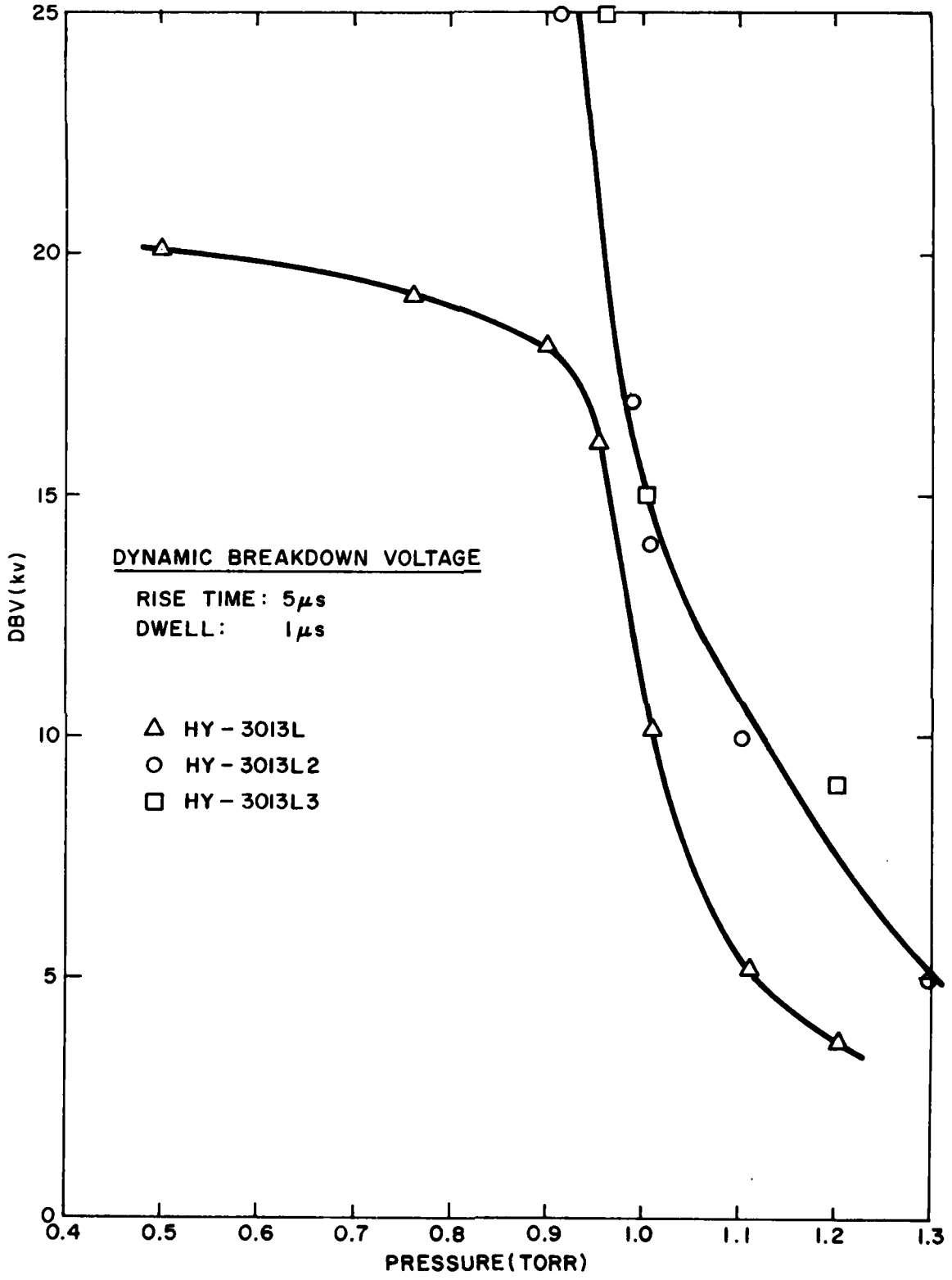

Figure 3. Dynamic breakdown voltage vs pressure.

of saturable reactor material required, and hence lowers the inductance of the saturable reactor section.) Saturable reactors are discussed in Section 5.

b. Recovery

During the recovery measurements it was determined that the long and erratic recovery times reported for HY-3013L (see Second Interim Report, p. 15), were caused by false triggering of one of the TM-11A charging modules, and not by actual recovery failure. When false triggering was eliminated, recovery was rapid, as discussed below.

The circuit used to measure recovery time is diagrammed in Figure 4. It is designed to simulate a prr greater than 20 kHz. First, epy is applied by TM-11 No. 1, then the thyratron is triggered, and after a variable time delay epy is re-applied by TM-11A No. 2. If the thyratron has recovered, the 150 pF capacitor re-charges to full epy and then discharges exponentially through the 100 kohm resistor. If the thyratron has not recovered, it conducts a second time even though no second trigger is applied, so that the 150 pF capacitor discharges abruptly either before or shortly after reaching epy.

Two TM-11As are required to simulate prr = 20 kHz because the open circuit output voltage of each one alone drops rapidly for prr greater than a few Hz. If TM-11A No. 2 false triggers when the thyratron first fires, then it is not able to put out any voltage when commanded to fire a few microseconds later. The 150 pF capacitor does not re-charge, just as if the thyratron had failed to recover.

Although the erratic nature of the recovery data aroused suspicion, this effect was not discovered immediately because its variation with epy, time delay, and thyratron pressure was qualitatively the same as recovery failure.

Circuit modifications to reduce false triggering included isolation resistors on the terminals of TM-11A No. 2, physical separation of circuit components, and liberal use of baluns and 50 ohm terminations. While these measures did not eliminate false triggering completely, they were successful enough to allow reliable recovery data to be taken.

Figure 5 shows recovery time t_r vs pressure for both HY-3013L and HY-3013L2. The HY-3013L data agree with the data given in Figure 7 of the First Interim Report. The faster recovery of HY-3013L2 is due to the smaller E-E space, as discussed in the Second Interim Report.

Recovery is fast enough for 20 kHz operation (t_r = 50 μs), up to a pressure of about 0.85 torr for HY-3013L, and 0.95 torr for HY-3013L2. Since load voltage rise rates of 6 kv/ns have been demonstrated at 0.7 torr (Second Interim Report,

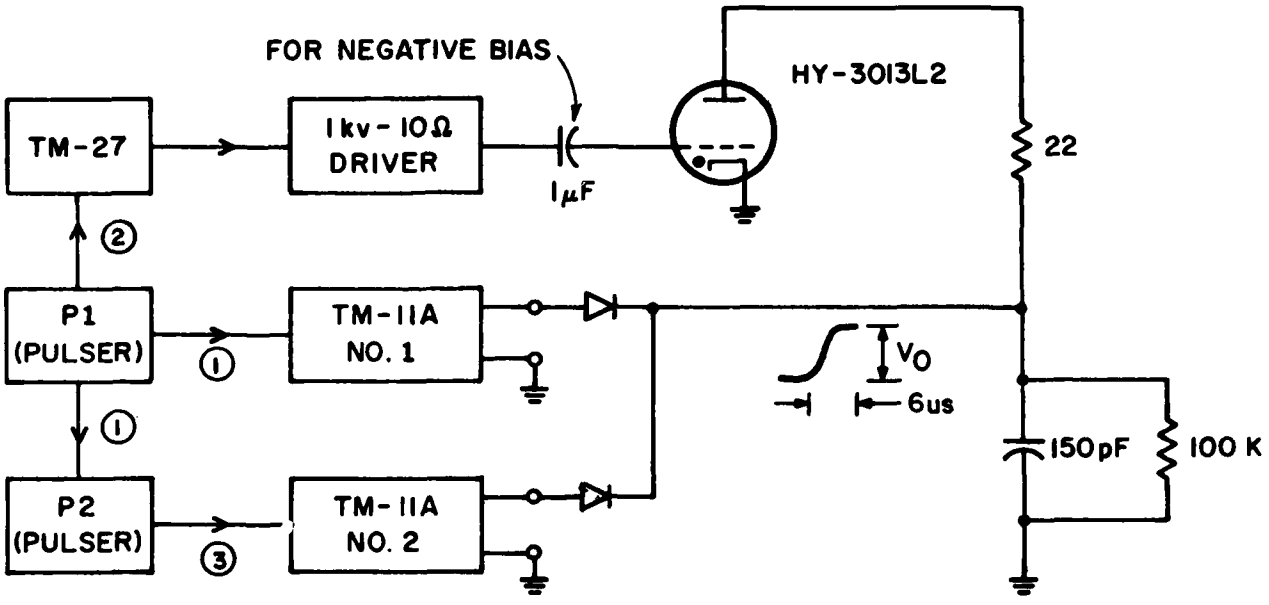

Sequence of Events:

1. Pulser P1 triggers TM-11A No. 1 which charges 150 pF to V_0. Simultaneously P1 triggers P2.

2. A delayed pulse from P1 triggers TM-27 which in turn triggers a 1 kv-10 driver, which triggers HY-3013L about 2 μs after the 150 pF reaches V_0.

3. Some time after HY-3013L2 fires, P2 triggers TM-11A No. 2 re-charging 150 pF to V_0, provided the time interval between ② and ③ is greater than the HY-3013L2 recovery time.

Figure 4. Circuit for recovery time measurements.

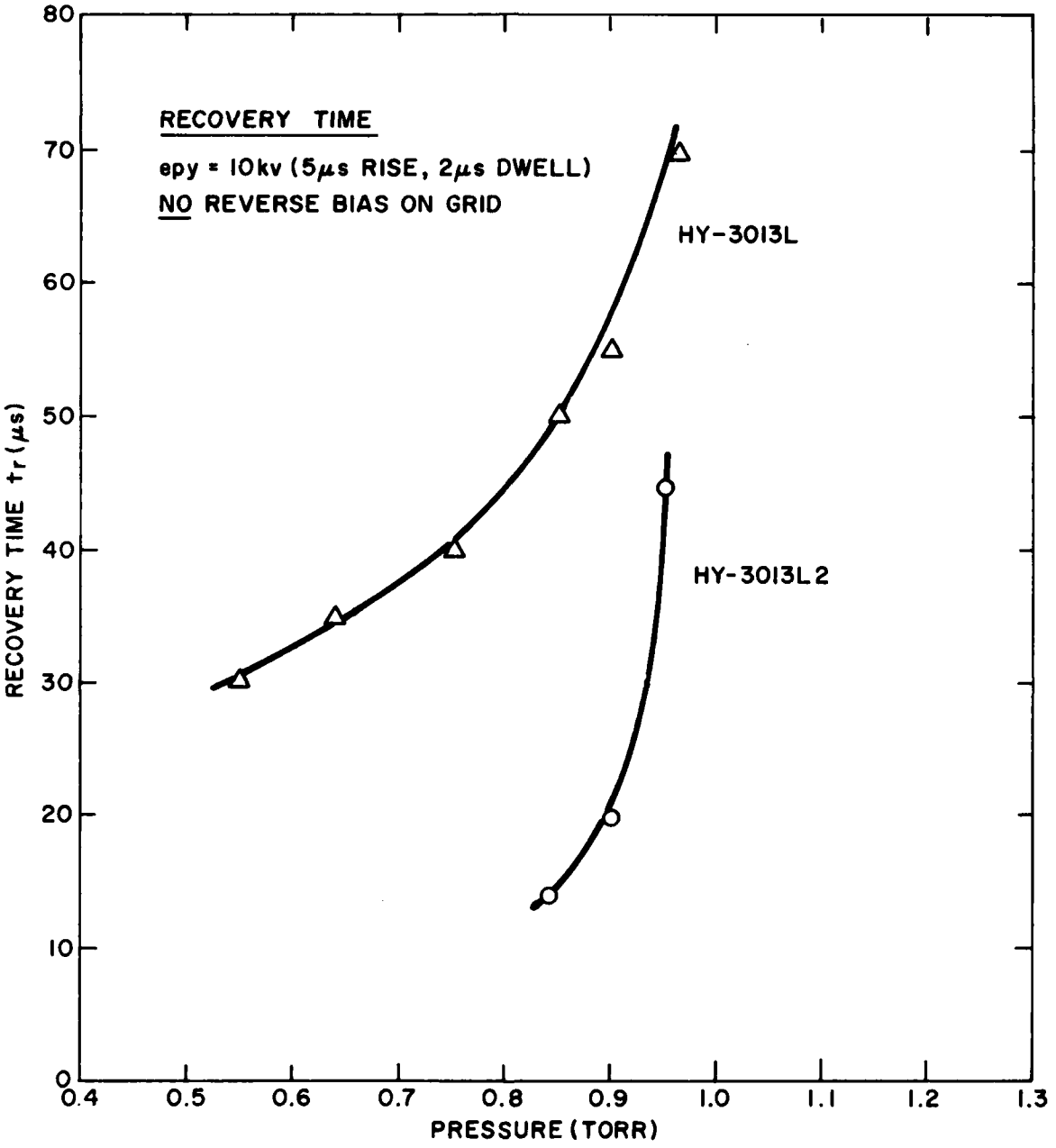

Figure 5. Recovery time.

Section 3), these recovery characteristics are more than adequate for the ultimate application.

Further shortening of t_r resulted when negative bias was applied to the control grid, accomplished by inserting a 1 μF capacitor between the trigger source and control grid.* Typical triggering conditions for HY-3013L2 were 450 volts egy superimposed on -150 volts negative bias.

With negative bias, t_r for HY-3013L2 was less than 15 μs at all pressures, and for all epy up to about 80% of DBV. (Recovery times shorter than 15 μs could not be measured because the width of the trigger pulse was nearly 15 μs.) All recovery measurements were made at peak currents, ib, of 400 amps.

Negative bias produced similar results in HY-3013L, although the measurements were more difficult because HY-3013L was hard to trigger when negative bias was applied.

Though the recovery characteristics of HY-3013L3 have not been measured, they should be similar to those of HY-3013L2.

c. Thyratron Trigger Requirements

Commutation with low trigger power is desirable not only from the point of view of overall system volume and power consumption, but also because it is usually associated with low jitter.

Trigger modules were available having output impedances of 200, 100, 50 and 10 ohms. While all four modules were able to break down the auxiliary grid of HY-3013L at voltages below 1 kv, the tube failed to commutate with the 100 and 200 ohm drivers. When reverse bias was used (to increase the recovery speed), only the 10 ohm trigger yielded reliable commutation.

HY-3013L2 was nearly as difficult to trigger, despite the absence of an auxiliary grid. The 50 ohm trigger sufficed even when reverse bias was applied, but commutation could not be obtained under any conditions with higher impedance triggers.

During this time, one of the newer production thyratrons (HY-8) was found to have exceptionally low jitter,[1] and to be easy to trigger, due to the unusually small offset between the apertures in adjacent electrodes (0.025 inch, as compared to 0.080 for HY3013L2 and 0.100 for HY-3013L).

---

*Each time the grid is triggered, some electrons hit the grid and flow to the grid side of the 1 μF capacitor. In between pulses, both grid and driver are open circuits, so these electrons accumulate until there are enough to repel further buildup. The result is a dc negative bias on the control grid.

Thyratron HY-3013L3 was therefore constructed with the same aperture offsets and inter-electrode spacings as the HY-8 (Figure 2c), resulting in a tube which commutated readily with a 200 ohm driver, even with reverse bias. Furthermore, the voltage holdoff was equal to that of HY-3013L2 (Figure 3).

d. Dispenser Cathode Development

Two 3-inch-diameter tetrode thyratrons of the HY-3006 type have operated successfully with a dispenser cathode for over 100 hours. The operating parameters and characteristics are similar to those of a standard-cathode HY-3006, as shown below.

HY-3006 Operating Characteristics

Parameters	Standard Cathode	Dispenser Cathode
Cathode Heater Voltage	6.3 V	6.3 V
Hydrogen Pressure	450 μ	450 μ
Anode Voltage	25-30 kv	30 kv
Peak Current	1.5-2 ka	1.5 ka
DC Average Current	1.5-2 A	2 A
Keep-Alive Current	50-200 mA	50 mA
Jitter	2 ns	3 ns
Anode Delay Time	50-100 ns	40 ns
Trigger Source	TM-29	TM-29

The dispenser cathode being used fits equally well into an HY-3013 type thyratron. A dispenser cathode HY-3013L can therefore be made at any time, but it would be best to await completion of more extensive tests with production tubes, and development of ultra-low inductance cathode-mounting designs.

4 LOAD AND PFN DEVELOPMENT

The test load should consist of a 30 pF capacitor shunted by a resistor. It has been determined theoretically and experimentally that a 4 ns FWHM voltage pulse can be applied across the load if the storage capacitor is ~240 pF, the load resistor is ~13 ohms, and the total circuit inductance (including the switch), is 17 nH or less.

In addition, the load and PFN must be rated for at least 150 watts average power (5 kv across 13 ohms, at a prr of 20 kHz and a pulse width of 4 ns).

To simplify construction, the load and PFN configuration was developed using a very short air gap having negligible inductance for a switch. Since the thyratron is ultimately expected to have an inductance of 8 nH, the desired load/PFN inductance was 9 nH or less.

After some experimentation, the configuration of Figure 6 was derived. Storage capacitor C_0 consisted of 10 mils of kapton sandwiched between aluminum plates. Resistor R was a disc of pressed ceramic, rated at 180 watts average power and 10 ohms. Load capacitance C consisted of the capacitance between this resistor and ground, through mylar dielectric. (In the final circuit, described in Section 6, the mylar is replaced by transformer oil, and the air gap by a thyratron.)

The voltage pulse across R produced in this assembly is shown in Figure 5c. Even though C_0 and C were greater than necessary (300 pF and 80 pF as compared to 240 pF and 30 pF), a 3.5 ns FWHM pulse was produced, having an amplitude approximately half that of the initial voltage on C_0.*

The overall inductance, estimated from the voltage waveform is 7 nH. (FWHM $\approx 2\sqrt{L(C_0 + C)}$.)

Reducing the total capacitance to 240 + 30 = 270 pF, and adding an 8 nH thyratron scales the FWHM to 4 ns. If the top 3.5 kv of a 5 kv pulse were used, the effective FWHM would become, assuming the same shape pulse as in Figure 6c, about 1.7 ns.

---

*Hence the statement in Section 2 that the thyratron voltage should be double the voltage to be applied to the load.

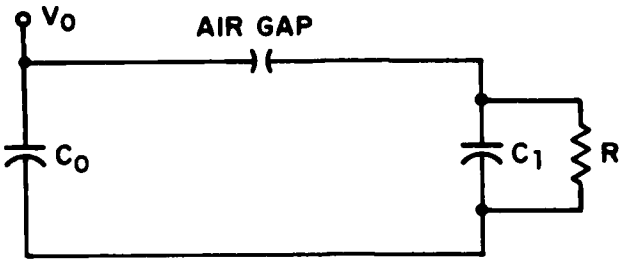

(a) Circuit schematic. C_0 initially charged to voltage V_0. C_1 and R constitute load.

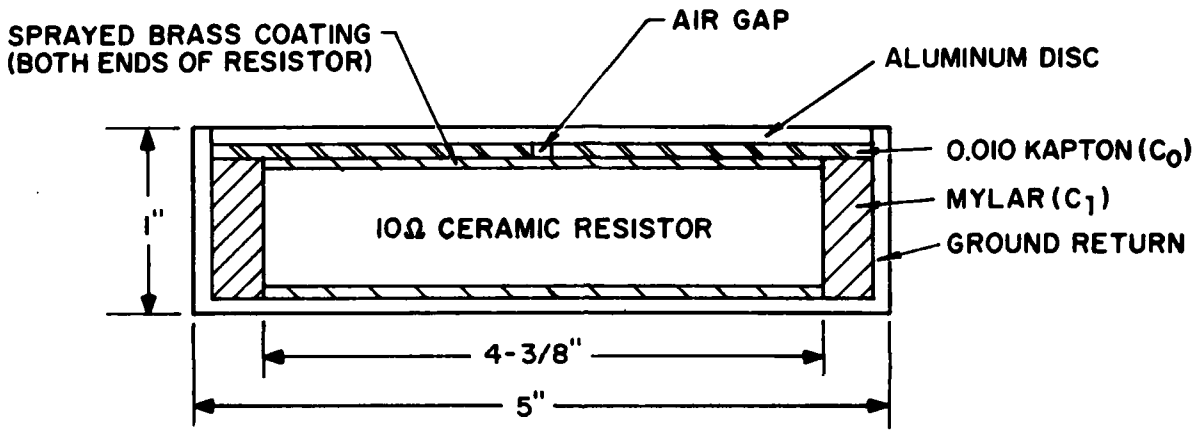

(b) Circuit assembly. C_0 is between aluminum disc and resistor. C_1 is between resistor O.D. and ground.

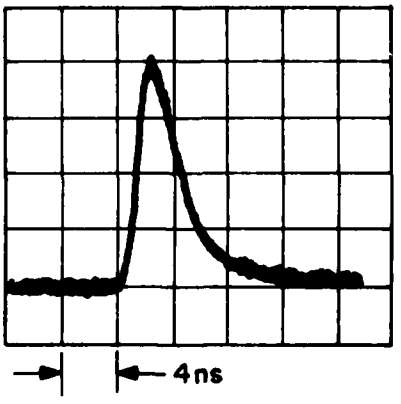

(c) Voltage across ceramic resistor (load voltage). Measured capacitances were C_0 = 300 pF, C_1 = 80 pF. Peak load voltage = 2.2 kv. V_0 = 4.3 kv.

Figure 6. Low inductance PFN/load circuit.

5 SATURABLE REACTOR DEVELOPMENT

a. Ferrite Reactor Design

A saturable reactor will be used to delay the current rise until the thyratron resistive fall is over. This will be necessary not only to sharpen the load voltage pulse, but also to reduce the thyratron anode dissipation which would otherwise be severe.

The saturable reactor section will be coaxial, as shown in Figure 7. The dimensions must necessarily be a compromise among three factors: current delay time, saturation current, and inductance.

Current delays of several nanoseconds require a large magnetic cross section, lw, which can only be achieved by making l large since w must remain small to ensure that the entire reactor saturates simultaneously. A low saturation current requires a small diameter, d. Low inductance, however, requires small l and large d.

Orthonol and metglas are attractive as saturable reactor materials because their low coercive force permits large diameter configurations with low saturation currents. However, low resistivity renders metglas unsuitable, and orthonol only a marginal possibility, as discussed in subsection 5.b.

We have, therefore, chosen ferrites. While the basic viability of ferrite beads was demonstrated by data presented in the Second Interim Report, their high coercive force may necessitate some tradeoff between anode dissipation (which increases with saturation current), and pulse width (which increases with inductance).

Since our work to date has concentrated on achieving the pulse width specifications, the initial saturable reactor design will aim for low inductance (about 1 nH), with a high saturation current (100 amps). The diameter will then be reduced as much as possible without significantly exceeding the inductance required for a 4 ns pulse width. Likely starting dimensions are d = 1.5 inches, l = 1 inch.

b. Evaluation of Orthonol and Metglas as Saturable Reactor Materials

In order to have a back-EMF comparable to epy during thyratron anode fall time t_f, followed by saturation at time $t = t_f$, the saturation flux density, B_s, and the magnetic area, A_m, of the saturable reactor must roughly satisfy

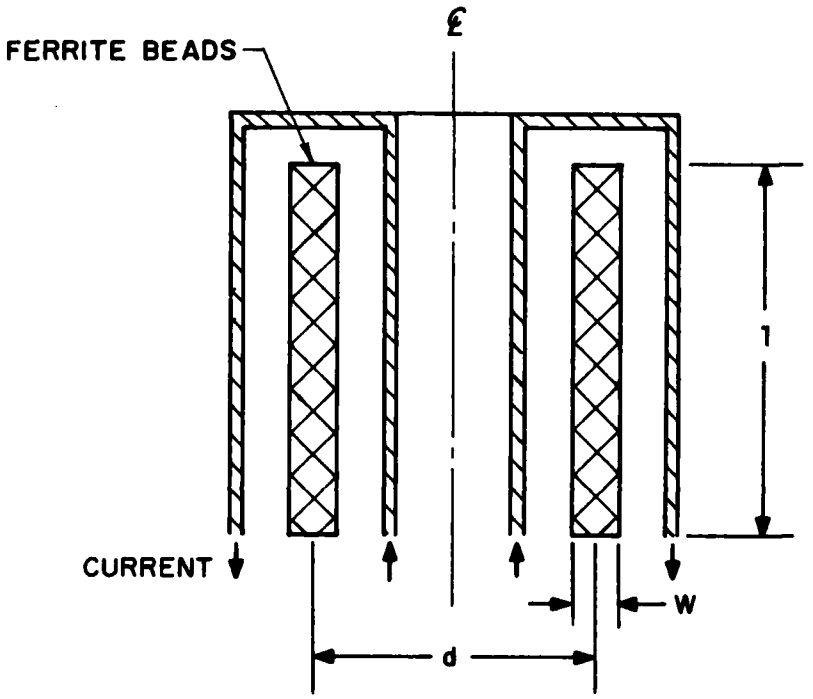

Figure 7. Coaxial saturable reactor using ferrites.

$$epy = \frac{A_m(t_f)B_s}{f} \tag{1}$$

If we assume a coaxial saturable reactor section of length l, then $A_m(t_f) = lx(t_f)$, where $x(t_f)$ is the penetration depth of saturation "front" at $t = t_f$. Equation (1) becomes

$$x(t_f) = epy \frac{t_f}{lB_s} \tag{2}$$

Following Nunally,[2] we assume shock-like propagation of the saturation front and get, approximately,

$$x(t_f) \approx \left[t_f \frac{\rho}{B_s} \frac{i(t_f)}{\pi d} \right]^{\frac{1}{2}} \tag{3}$$

where is the resistivity, $i(t_f)$ the circuit current at $t = t_f$, and d the average diameter of the saturable reactor configuration.

The problem with orthonol and metglas is that their resistivity is too low for $x(t_f)$, as calculated from Equation (3), to satisfy the condition of Equation (2). This will now be shown.

The following parameter values apply:

epy = 10,000 volts
t_f = 10^{-8} second
B_s = 1.6 webers/m^2
l = 0.1 meter maximum for reasonably low inductance
d = 0.05 meter minimum for reasonably low inductance
ρ = 50 x 10^{-8} ohm-m for orthonol
ρ = 125 x 10^{-8} ohm-m for metglas
$i(t_f)$ = 100 amps maximum (10-20% of ultimate peak current).

These give, from Equation (2), a required $x(t_f)$ of 0.625 x 10^{-3} meter, or 25 mils.

From Equation (3), we get $x(t_f)$ = 0.056 mil for orthonol, and 0.089 mil for metglas.

Therefore, in order to achieve the required $x(t_f)$, we would need to wrap approximately $\frac{1}{2}$ x 25/0.089 ~ 140 laminations of metglas, or 225 laminations of orthonol. (The factor $\frac{1}{2}$ is present because the magnetic field penetrates from both sides of the lamination.)

Winding such a large number of laminations would be difficult, especially considering the sensitivity of the magnetic properties of orthonol and metglas to handling.

However, even if we succeeded in constructing such windings, they would still not work under our conditions because the minimum available thicknesses of orthonol and metglas are too great for saturation to be complete by $t = t_f$.

The thinnest obtainable metglas is 1 mil, giving, from Equation (3), a saturation time of 2.3 μs. At an $i(t_f)$ of 100 amperes, all the charge in the energy storage capacitor would be drained off by the time the reactor saturated.* Thus, metglas is not a viable saturable reactor material for this application.

The thinnest obtainable orthonol is 1/8 mil, giving a saturation time of 50 ns. The charge drained off the energy storage capacitor at $t = t_f$ would be 2.5 x 10^{-6} coulomb, essentially all the charge stored. Increasing epy to compensate is possible but undesirable from a thyratron holdoff viewpoint, and increasing the storage capacitance to compensate would increase the ultimate load voltage pulse width. Therefore, orthonol must be considered as only marginally feasible as a saturable reactor material for this application.

Given the aforementioned practical difficulties involved in winding a suitable orthonol reactor, we will continue to use ferrite beads for the present. Ferrite beads are highly resistive, so the field penetration is effectively instantaneous, and they are also convenient to use.

---

*240 pF x 10,000 volts = 2.5 x 10^{-6} coulomb. Assuming a linear current rise, $\frac{1}{2}$ x 100 amps x 1.3 μs = 6.5 x 10^{-5} coulomb.

6 OVERALL CIRCUIT DESIGN

The complete nanosecond pulser circuit is diagrammed schematically and pictorially in Figure 8. The entire assembly will be immersed in transformer oil for insulation.

Cooling of the saturable reactor section (which must be kept below the 150°C Curie temperature of the ferrites), will be promoted by its being located at an end of the assembly, and by its proximity to the large aluminum top piece. If necessary, this piece can be contoured and/or finned for better cooling.

Parts for the circuit assembly are currently on order.

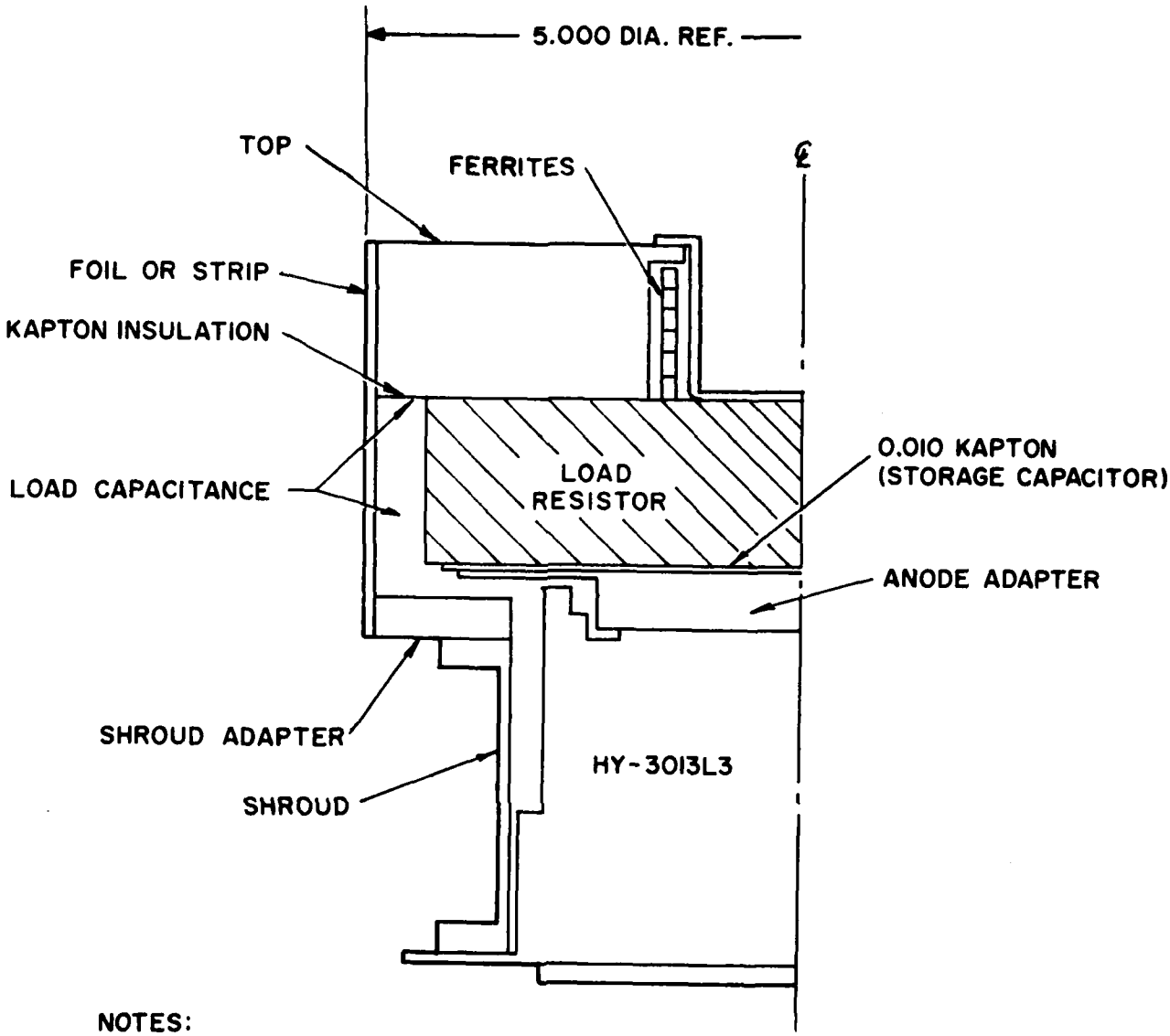

NOTES:

1. TO BE IMMERSED IN TRANSFORMER OIL.

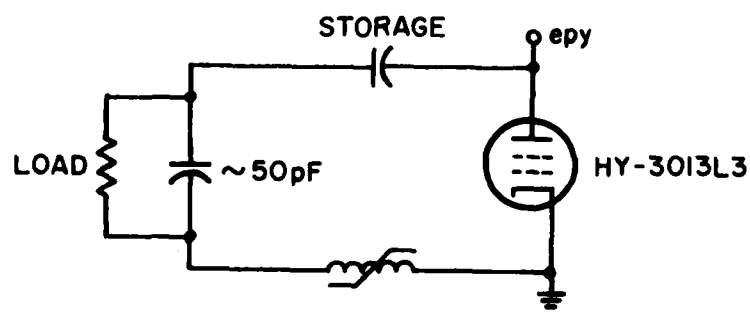

Figure 8. Circuit assembly.

7 20 kHz TEST KIT

The 20 kHz test kit, diagrammmed schematically in Figure 9, is designed to command charge 500 pF to 20 kv with a 3 μs rise time. The kit is now complete and ready for final checkout.

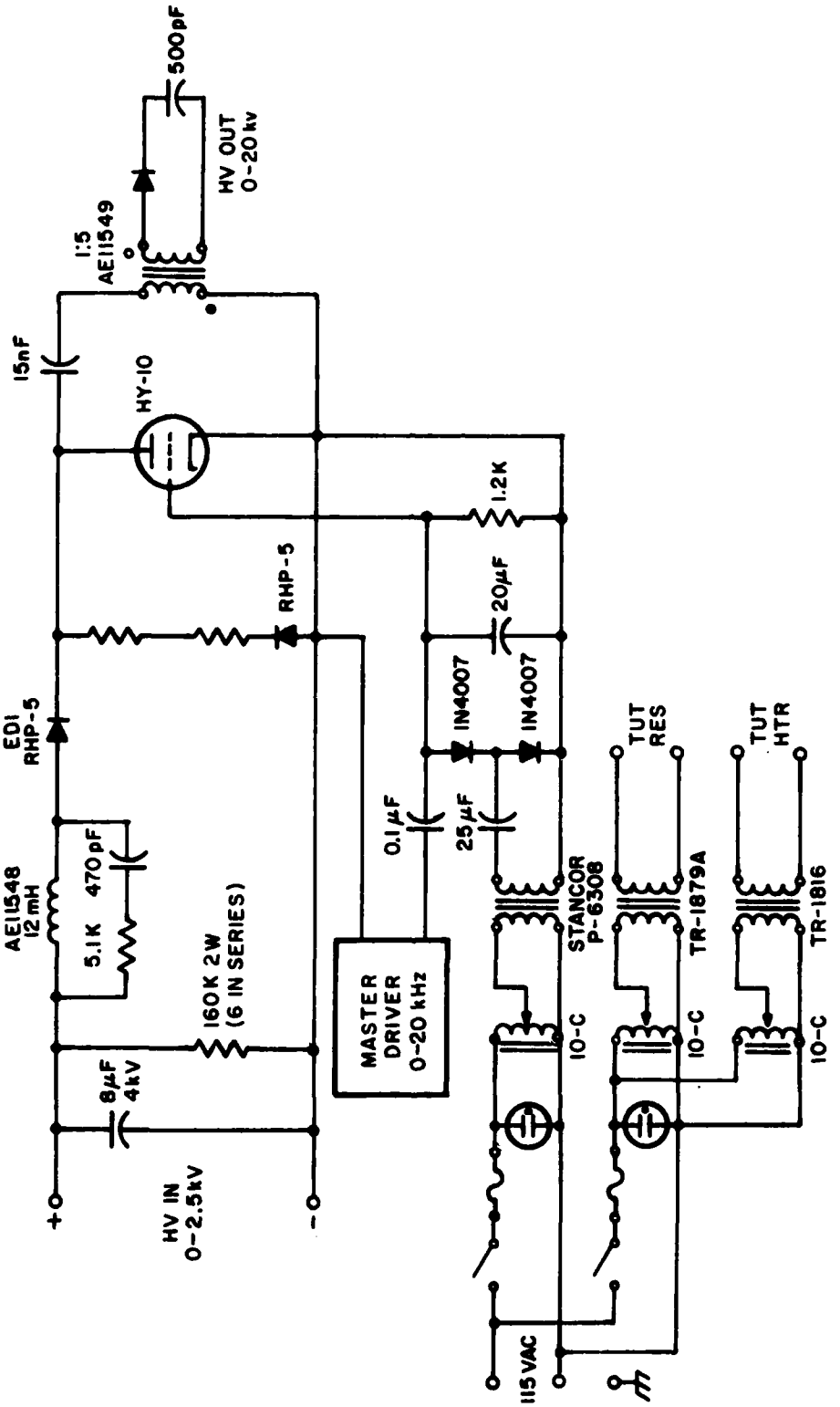

Figure 9. 20 kHz test kit.

8 FUTURE PLANS

The circuit of Figure 8 will be assembled, tested at low prr and, if necessary, modified until the desired load voltage pulse is produced, after which high prr testing will commence.

9 REFERENCES

(1) Krausse, G.J., and Sarjeant, W.J., 3rd IEEE Int. Pulsed Power Conf., Albuquerque, New Mexico, June 1-3, 1981.

(2) Nunally, W.C., Los Alamos National Laboratory Report, LA-8862-MS, May 1981. (Rough draft) Eqn. 30.

ELECTRONICS TECHNOLOGY AND DEVICES LABORATORY
MANDATORY CONTRACT DISTRIBUTION LIST

101 Defense Technical Information Center
ATTN: DTIC-TCA
Cameron Station (Bldg 5)
012 Alexandria, VA 22314

203 GIDEP Engineering & Support Dept
TE Section
PO Box 398
001 Norco, CA 91760

205 Director
Naval Research Laboratory
ATTN: CODE 2627
001 Washington, DC 20375

301 Rome Air Development Center
ATTN: Documents Library (TILD)
001 Griffiss AFB, NY 13441

437 Deputy for Science & Technology
Office, Asst Sec Army (R&D)
001 Washington, DC 20310

438 HQDA (DAMA-ARZ-D/Dr. F.D. Verderame)
001 Washington, DC 20310

432 Director
US Army Materiel Systems Analysis Actv
ATTN: DRXSY-MP
001 Aberdeen Proving Ground, MD 21005

563 Commander, DARCOM
ATTN: DRCDE
5001 Eisenhower Avenue
001 Alexandria, VA 22333

564 Cdr, US Army Signals Warfare Lab
ATTN: DELSW-OS
Vint Hill Farms Station
001 Warrenton, VA 22186

567 Command Commandant
U.S. Army Engineers School
ATTN: ATZA-TDL
002 Ft. Belvoir, VA 22060

569 Commander
U.S. Army Engineer Topographic Labs
ATTN: ETL-TD-EA
001 Ft. Belvoir, VA 22060

602 Cdr, Night Vision & Electro-Optics
ERADCOM
ATTN: DELNV-D
001 Fort Belvoir, VA 22060

603 Cdr, Atmospheric Sciences Lab
ERADCOM
ATTN: DELAS-SY-S
001 White Sands Missile Range, NM 88002

607 Cdr, Harry Diamond Laboratories
ATTN: DELHD-CO, TD (In Turn)
2800 Powder Mill Road
001 Adelphi, MD 20783

609 Cdr, ERADCOM
ATTN: DRDEL-CG, CD, CS (In Turn)
2800 Powder Mill Road
001 Adelphi, MD 20783

612 Cdr, ERADCOM
ATTN: DRDEL-CT
2800 Powder Mill Road
001 Adelphi, MD 20783

680 Commander
US Army Electronics R&D Command
000 Fort Monmouth, NJ 07703
1 DELET-MQ
1 DELEW-D
1 DELET-DD
1 DELSD-L (Tech Library)
2 DELSD-L-S(STINFO)
25 Originating Office
1 DELET-MF

681 Commander
CECOM
000 Ft. Monmouth, NJ 07703
1 DRSEL-PL-ST
1 DRSEL-COM-BO
1 USMC-LNO
1 ATFE-LO-EC
1 DRSEL-MA-MP
1 DRSEL-PA
1 DRSEL-LG-L

SUPPLEMENTAL CONTRACT DISTRIBUTION LIST
(ELECTIVE)

103 Code R123, Tech Library
DCA Defense Comm Engrg Ctr
1800 Wiehle Avenue
001 Reston, VA 22090

207 Cdr, Naval Surface Weapons Center
White Oak Laboratory
ATTN: Library Code WX-21
001 Silver Spring, MD 20910

403 Cdr, MICOM
Redstone Scientific Info Center
ATTN: Chief, Document Section
001 Redstone Arsenal, AL 35809

407 Director, Ballistic Missile Defense
Advanced Technology Center
ATTN: ATC-R, PO Box 1500
001 Huntsville, AL 35807

475 Cdr, Harry Diamond Laboratories
ATTN: Library
2800 Powder MIll Road
001 Adelphi, MD 20783

477 Director
US Army Ballistic Research Labs
ATTN: DRXBR-LB
001 Aberdeen Proving Ground, MD 21005

*481 Harry Diamond Laboratories
ATTN: DELHD-RCB
(Dr. J. Nemarich)
2800 Powder Mill Road
001 Adelphi, MD 20783

507 Cdr, AVRADCOM
ATTN: DRASAV-E
PO Box 209
001 St. Louis, MO 63166

511 Commander, Picatinny Arsenal
ATTN: SARPA-FR-5, -ND-A-4, -TS-S (In Turn)
001 Dover, NJ 07801

519 Cdr, US Army Avionics Lab
AVRADCOM
ATTN: DAVAA-D
001 Fort Monmouth, NJ 07703

531 Cdr, US Army Research Office
ATTN: DRXRO-PH (Dr. Lontz)
DRXRO-IP (In Turn)
PO Box 12211
001 Research Triangle Park, NC 27709

614 Cdr, ERADCOM
ATTN: DRDEL-LL, -SB, -AP (In Turn)
2800 Powder Mill Road
001 Adelphi, MD 27083

617 Cdr, ERADCOM
ATTN: DRDEL-AQ
2800 Powder Mill Road
001 Adelphi, MD 20783

619 Cdr, ERADCOM
ATTN: DRDEL-PA, -ILS, -ED (In Turn)
2800 Powder Mill Road
001 Adelphi, MD 20783

701 MTI - Lincoln Laboratory
ATTN: Library (RM A-082)
PO Box 73
002 Lexington, MA 02173

*For Millimeter & Microwave Devices Only

SUPPLEMENTAL CONTRACT DISTRIBUTION LIST (CONT.)
(ELECTIVE)

General Electric Company
Electronics Lab
Electronics Park
Syracuse, NY 13201
ATTN: Mr. S. Wanuga (1)

Air Force Cambridge Labs
ATTN: CRDR (Dr. P. Carr &
Dr. A.J. Slobodnik)
Bedford, MA 01730 (2)

Dr. Tom Bristol
Hughes Aircraft Company
Ground Systems Group
Bldg 600/MS D235
1901 W. Malvern
Fullerton, CA 92634 (2)

Raytheon Company
Research Division
28 Seyon Street
Waltham, MA 02154
ATTN: Dr. M.B. Schulz (1)

Sperry Rand Research Center
100 North Road
Sudbury, MA 01776
ATTN: Dr. H. Van De Vaart (1)

Microwave Laboratory
W.W. Hansen Laboratories of Physics
Stanford University
Stanford, CA 94305
ATTN: Dr. H.J. Shaw (2)

APPENDIX
LUMPED CIRCUIT ANALYSIS

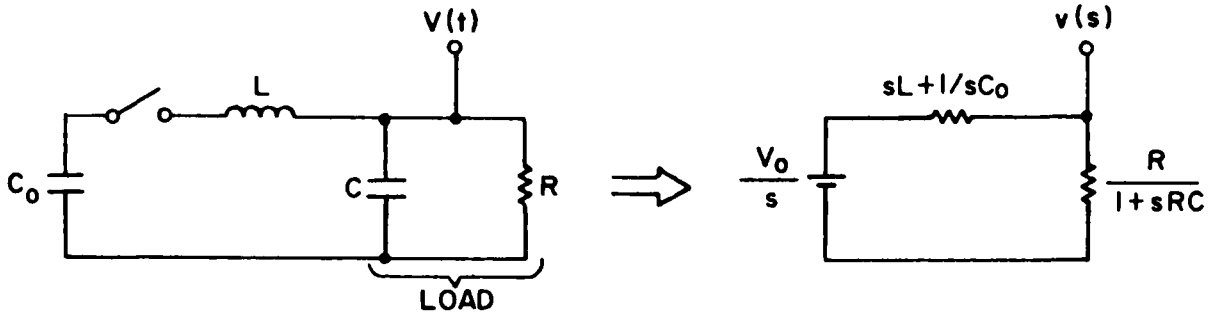

$$\frac{v(s)}{V_0} = \frac{1}{s} \frac{R/(1 + sRC)}{sL + \frac{1}{sC_0} + \frac{R}{1 + sRC}} = \frac{1}{s^3LC + s^2 \frac{L}{R} + s\left(1 + \frac{C}{C_0}\right) + \frac{1}{RC_0}} \qquad \text{(B-1)}$$

$$LC \frac{v(s)}{V_0} = \frac{1}{s^3 + \frac{1}{RC} s^2 + \frac{1 + C/C_0}{LC} s + \frac{1}{RLCC_0}} \qquad \text{(B-2)}$$

For critical damping this should have the form

$$LC \frac{v(s)}{V_0} = \frac{1}{(s + \alpha)^3} \qquad \text{(B-3)}$$

This requires that "α" satisfy three conditions:

$$3\alpha = \frac{1}{RC} \qquad \text{(B-4)}$$

$$3\alpha^2 = \frac{1 + C/C_0}{LC} \qquad \text{(B-5)}$$

$$\alpha^3 = \frac{1}{RLCC_0} \qquad \text{(B-6)}$$

Then

$$\boxed{\frac{V(t)}{V_0} = \frac{3}{2} \frac{1}{1 + \frac{C}{C_0}} (\alpha t)^2 e^{-\alpha t}} \qquad \text{(B-7)}$$

Eliminating L and R from Equations (B-4), (B-5), and (B-6) gives $\frac{C_0}{C} = 8.$

$\text{FWHM} = \frac{3.4}{\alpha} = 10.2$ RC which for 4 ns and C = 60 pF gives R = 6.5 Ω. Returning to conditions (B-5) and/or (B-6) we get L = 8.7 nH.

The maximum value of $\frac{V(t)}{V_0}$ occurs at $\alpha t = 2$ and is equal to 0.7.